Registration of Brain Images With Tumors: Towards the Construction of Statistical Atlases for Therapy Planning

Evangelia I. Zacharaki, Dinggang Shen, Ashraf Mohamed, Christos Davatzikos

Section of Biomedical Image Analysis, Department of Radiology, University of Pennsylvania

ABSTRACT

A deformable registration method is proposed to register a brain atlas with tumor-bearing brain scans. The tumor mass effect is first simulated in the (normal) atlas, using a biomechanical model of mass effect. The tumor-bearing atlas is subsequently warped to the patient's scan by a deformable registration method, built upon the idea of HAMMER registration algorithm developed for normal brains. The potential of using the pattern of deformation around the tumor region to optimize the location of tumor seed and other parameters of the tumor model is also explored. Quantitative evaluation on simulated data shows that the proposed method achieves accuracy similar to that achieved in registration of images without tumors. Moreover, limited registration results on real tumors are promising.

1. INTRODUCTION

The overall goal of our study is to construct statistical atlases from images of brain tumor patients. These atlases can ultimately integrate a variety of patient data and link them to outcome measures. For example, patterns of progression of brain gliomas can be systematically investigated in large cohorts of patients via a variety of imaging methods (conventional MRI, perfusion, spectroscopy, DTI) with the goal of finding predictive imaging-based factors for tumor progression. Moreover, radiation dose distribution, tumor location relative to brain structures and outcome measures, can be integrated in order to elucidate relationships among these variables that can assist in radiotherapy and radiosurgical planning. To achieve this, a method that is able to register a stereotactic brain atlas with the patient images must be available. However, most of the available registration methods are designed to register a normal atlas with normal subjects. If directly applying those methods to tumor patient images, the registration around the tumor region can fail due to substantial image dissimilarities and deformations.

The proposed approach is designed based on the idea of decoupling the total deformation (between normal atlas and patient scan) into two basic components: (i) the tumor-induced deformation, which can be modeled by a tumor growth and mass effect model [1, 2]; (ii) the inter-subject deformation, which can be estimated by a registration algorithm. Similar approaches have already been investigated [3-7]. Some of these methods used a normal-to-normal brain matching method after shrinking the tumor in brains [3]. Some applied first an affine transformation between the normal atlas and the patient's image and subsequently either used a rich tumor simulation model of mass-effect and invasion without further accounting for the inter-subject differences [6], or used a simplified radial growth model refined by a non-rigid deformation based on optical flow [4, 5]. Other methods just combined the Talairach transformation with the simple radial expansion model [7] in order to speedup the algorithm.

In this paper, we focus on the image registration component of the proposed framework using an elastic feature-based registration method based upon the idea of HAMMER registration algorithm developed for normal brains [8]. One of the challenges here is to reliably establish anatomical correspondence in regions around the tumor, while maintaining good registration in the healthy brain anatomy.

2. METHODS

The proposed registration method is designed to have the following three properties. (i) It aims at determining anatomical correspondences if such correspondences exist, rather than matching image intensities; (ii) it is robust to slightly inaccurate estimates of the tumor simulation parameters; (iii) it aims at estimating the optimal parameters for the tumor growth model by examining the deformation pattern around the tumor — the hypothesis is that optimal tumor parameters minimize the discrepancy between the atlas with a tumor and the patient's images. For determining anatomical correspondences, an attribute vector is attached to each image voxel, aiming at distinctively summarizing the anatomical context around that voxel, including healthy and malignant tissue. For better robustness, we define a confidence level for tissue classification and introduce certain constraints in the calculation of the global component of deformation. Finally, for estimating optimal tumor growth parameters, we place special emphasis on the warping of the tumor neighborhood, such as modifying the strategy of selecting and focusing on salient points for registration in HAMMER [8]. We hope that the incorporation of several image-based and deformation-based criteria into a single evaluation measure will reveal

information about the accuracy of the proposed framework and more specifically the estimation of the tumor growth model parameters.

2.1. Tumor growth simulation

We use the nonlinear biomechanical model in [1, 2] to simulate tumor growth in the atlas. It should be noted that any other approach of modeling the impact of macroscopic tumor growth on the surrounding normal parenchyma could be used instead. The amount of tissue death is simulated by replacing a part of the brain parenchyma with a small tumor mass, whose location and size are parameters of the model (typically to be estimated from the patient's images). The possible initial peri-tumor edema is similarly defined by an edema mask spanning only over white matter regions. The mass effect of the tumor growth is modeled by applying a pressure normal to the initial tumor boundary and solved by the finite element method. The boundary conditions and the material properties complete this relatively basic model of mass effect and tissue death.

2.2. Registration method

The automatic elastic registration algorithm is applied on skull-stripped [9] and segmented images [10], which have been first linearly aligned [11]. It is based on a coarse to fine resolution scheme of three levels, following the general framework of the HAMMER algorithm [8]. At each resolution, the deformation field is calculated according to the hierarchical approximation of an energy function, which consists of a similarity matching criterion defined in the template space, a constraint on the inverse matching, and smoothness constraints on the displacement field.

An attribute vector, $\mathbf{a}(\mathbf{x}) = [\mathbf{a}_i(\mathbf{x})], i = 1,2,3$, is defined for each image voxel, reflecting edge information ($\mathbf{a}_1$), image intensity ($\mathbf{a}_2$), and geometric moment invariants ($\mathbf{a}_3^j$, $j = 1,..,K$) for each one of the K tissue types, respectively. In case of images with tumor, the attribute vector is enriched by introducing an additional attribute, $\mathbf{a}_4$, which reflects the signed distance from the tumor boundary. In the brain parenchyma, the features that drive the deformation are selected hierarchically according to the distinctiveness of their attributes, such as roots of sulci, crowns of gyri, or voxels located on strong and isolated edges. Moreover, driving voxels are selected in the areas around and very close to the tumor, which is denoted by V_T in template and V_S in subject, respectively. The tumor neighborhood changes according to a threshold, which is higher for lower resolutions due to the smaller number of driving voxels, i.e. 8, 4, 2*mm* for the low, middle and high resolution, respectively. At each resolution, the threshold also slightly increases during the hierarchical registration procedure, thus obtaining more driving voxels from the healthy brain tissue around the tumor. The similarity of two voxels $\mathbf{x}$ and $\mathbf{y}$ is defined as

$$Sim(\mathbf{x},\mathbf{y}) = \begin{cases} \left(1 - \left|\mathbf{a}_4(\mathbf{x}) - \mathbf{a}_4(\mathbf{y})\right|\right), & if \quad \mathbf{x} \in V_T \quad or \quad \mathbf{y} \in V_S \\ m(\mathbf{x},\mathbf{y}), & otherwise \end{cases}$$

$$m(\mathbf{x},\mathbf{y}) = \begin{cases} 0, & if \ \mathbf{a}_1(\mathbf{x}) \neq \mathbf{a}_1(\mathbf{y}) \\ \left(1 - \left|\mathbf{a}_2(\mathbf{x}) - \mathbf{a}_2(\mathbf{y})\right|\right) \cdot \prod_{j=1}^{K} \left(1 - \left|\mathbf{a}_3^j(\mathbf{x}) - \mathbf{a}_3^j(\mathbf{y})\right|\right), & otherwise \end{cases} \quad (1)$$

The optimal correspondence is determined by integrating the similarity of the attribute vectors within a small volume around each driving voxel, accounting for the lack of distinctiveness of the attribute $\mathbf{a}_4$ in voxels with the same distance from tumor.

The correspondence of driving voxels determined above is interpolated elsewhere via a Gaussian kernel function, in conjunction with a Laplacian-based smoothing that reduces with time as the level of confidence in estimating tumor parameters, θ, increases. Additional to the local smoothness constraints, global constraints are also applied, based only on point correspondences lying in the regions of high confidence. If the estimation of θ is accurate, the displacement field in the region around the tumor is expected to be smooth, and conversely.

2.3. Estimating θ from deformation around the tumor

As we mentioned above, the pattern of deformation around the tumor can be indicative of the accuracy in estimating the parameters of the tumor model, θ. If θ is wrong, and thus tumor is incorrectly simulated in the atlas, unrealistic and severe deformations are expected around the tumor region, when trying to match the atlas with the patient's image. Conversely, if the estimations of tumor location and mass effect in the atlas are in agreement with those in the patient, a relatively smooth deformation should be obtained. In this section, we briefly describe an attempt to utilize the characteristics of the deformation field as well as the anatomical characteristics of the co-registered images around the tumor for refining our estimate of θ. The estimation error E_θ, given θ, is calculated in a volume Ω, defined in the subject brain within a specific distance r from tumor ($r \approx 15\ mm$). It is the linear combination of four normalized measures M_i

$$E_\theta = \sum_i \frac{a_i}{V_i} \sum_{x \in V_i} M_i(\mathbf{x};\theta) \ , \ i = 1,...,4 \quad (2)$$

where a_i is a weighting parameter for each measure, and $V_i \subseteq \Omega$ is the volume over which each measure is calculated. The weighting parameters are currently determined experimentally. M_1 and M_2 are defined to reflect the similarity of co-registered atlas and patient's images and the similarity of their attribute vectors, respectively. M_3 and M_4 are defined to reflect smoothness properties of the deformation field itself, using the Jacobian determinant and the Laplacian, respectively. The details are omitted due to space limitations.

3. RESULTS

The registration method has been evaluated in three different cases: (i) both the variation in the anatomy and the deformation caused by tumor growth are simulated and thus can be used as gold-standards, (ii) tumor growth is simulated in a real MR dataset, (iii) a normal atlas is registered with a real patient's scan. The first two cases are designed to quantitatively assess the registration accuracy by manually placing the tumor seed in the correct or in wrong tumor locations. Concerning the real case where θ is unknown, tumor growth is simulated using three different sets of θ and then the best θ is chosen by visually evaluating the registration result for every one of them. This part will be performed automatically in the future by using as evaluation function the estimation error E_θ proposed in Section 2.3. The applicability of E_θ in optimizing the tumor growth parameters is investigated in the Section 3.4 of the results.

Hereby we would like to notice that although the proposed framework has been applied to monofocal tumor growth, it can easily be extended to cases with multiple lesions. However such an extension might be redundant, because such lesions are usually very small and their mass effect can be ignored. Thus, a normal brain registration method might also be suitable.

3.1. Simulated brain deformation and tumor growth

Anatomical deformation is simulated by the method in [12], to create a synthesized brain from a template brain. Then, tumor growth is simulated in both template and synthesized brains in the corresponding locations. The latter is treated as the tumor-diseased subject. The procedure has been repeated twice using two different pressures to produce tumors of medium size and large size. For both pressure values, we have calculated the root-mean square (*rms*) and the maximum (*max*) error from the tumor-bearing subject to the normal template between the deformations simulated and the deformation estimated by our framework. The calculation is separately performed over the tumor neighborhood Ω and the rest of the brain. The results are given in Table 1. For comparison, the HAMMER algorithm is used to warp the normal synthesized brains (without tumors), yielding an *rms* error 0.797*mm* and a *max* error 6.470*mm*. It can be observed that the presence of tumor does not drastically reduce the registration accuracy in the brain regions that are not close to the tumor (Table 1, 2nd row), compared to the performance of HAMMER in registering the normal synthesized brains. A small amount of error increase is reasonable, given the interpolation errors due to the transition between the 3D cubic mesh and the finite element mesh used for the tumor model. Moreover, as expected, the *rms* error increases in Ω with increase of tumor size, which is more than that in the rest of the brain. Fig.1 shows the warping result for the tumor-deformed template with large pressure by correct estimation of tumor parameters, θ_0. The superimposition of subject edges on the template image shows the visible improvement after deformable registration.

Table 1. Registration accuracy on simulated data by correct estimation of tumor growth parameters (θ_0).

domain	*medium pressure*		*large pressure*	
	rms	*max*	*rms*	*max*
Ω	2.139	5.930	3.729	8.643
brain\Ω	1.157	7.035	1.181	7.296

In order to investigate the effect of tumor growth estimation, we simulated a tumor in the template image using the same initial seed and the medium pressure as before, but at six different locations (θ_1-θ_6) around the correct location (θ_0) in a distance ±6*mm* in each axis. Then, we warped each tumor-bearing template to the tumor-bearing subject. For the six locations, the *rms* error varied between 3.375*mm* and 5.068*mm* in tumor neighborhood Ω and between 1.154*mm* and 1.235*mm* in the rest of the brain. The *max* error has increased for all six locations (9.384 ~ 15.838*mm*), but was located inside the tumor region Ω. These results show that the proposed method is robust in the brain regions not close to the tumor, but sensitive around the tumor neighborhood. This is actually consistent with our expectation as indicated in Section 2.

3.2. Simulated tumor growth in real brains

This experiment evaluates the performance of the proposed method, based on manual landmarks, in registering two real brains where tumor growth is simulated in both of them. A set of locations, R_0, is first predefined in the real brain used as template. Then, two raters placed independently the corresponding landmarks, R_1 and R_2, in the second real brain, which is used as subject. The landmarks R_1 and R_2 are displaced according to the tumor-induced deformation in subject. Then, those displaced landmarks are registered to the tumor-bearing template with the proposed registration algorithm and subsequently mapped to the pre-tumor template by using the inverse tumor growth deformation, thus ideally matching with R_0. The minimum (*min*), average (*avg*), and maximum (*max*) landmark errors are computed, as shown in Table 2. The maximum error is quite large; however, the inter-rater variation in the normal subject (R_1R_2) is also very large.

(a) (b) (c) (d)

Fig. 1 Example of simulating tumor in a normal template with initial seed in (a) and warping it to a simulated tumor-diseased subject in (d). The white curves represent the edges of the tumor-diseased subject, and are overlaid on the template (b) before and (c) after registration.

Table 2. Landmark errors on a real brain with/without tumor using the proposed framework/HAMMER respectively.

	pairs	*min*	*avg*	*max*
Proposed framework	R_1R_2	0.938	5.188	19.691
	R_1R_0	0.940	8.241	18.463
	R_2R_0	0.791	6.680	16.262
HAMMER	R_1R_0	1.463	8.775	21.487
	R_2R_0	1.223	7.003	14.457

For comparison, HAMMER is used to map the landmarks in the two real normal brains (without tumor). It can be observed that registration accuracy is at the same level, thus indicating the ability of the proposed framework to compensate for the large tumor-induced deformations and image dissimilarities.

3.3. A real case of tumor-diseased brain

Tumor in normal template is roughly simulated by visually comparing the output of the simulation (Fig.2a) with the patient's image (Fig.2c). As previously mentioned, this part will be improved via an iterative scheme based on the minimization of E_θ, to be developed in future. The tumor-induced deformation is further refined by the proposed registration method to account also for the inter-subject variability. The high similarity between the warped tumor-simulated template (Fig.2b) and the patient's image can easily be observed.

3.4. Tumor parameter estimation

In order to test the potential of optimizing the estimation of tumor growth parameters, θ, preliminary results were obtained using the simulated data in Section 3.1 as they provide ground truth about θ. The medium pressure value has been applied and the four measures have been calculated as a function of θ. Table 3 shows that, after registering images with the proposed method, all four measures have the smallest value for the case of correct tumor parameter estimation (θ_0), thereby indicating the potential of using these measures for optimizing the estimation of θ. Our results in this section are quite preliminary, and must be further investigated in more datasets.

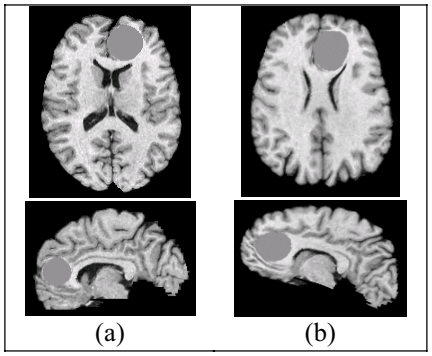

Fig.2. Example of a tumor-simulated template (a) before and (b) after warping to a real tumor-diseased brain in (c).

Table 3. Sensitivity of M_i as a function of θ.

	$\mathbf{M_1}$	$\mathbf{M_2}$	$\mathbf{M_3}$	$\mathbf{M_4}$	$\boldsymbol{E}$
$\boldsymbol{\theta_0}$	0.2239	0.4550	0.0062	0.0112	*0.1629*
$\boldsymbol{\theta_1}$-$\boldsymbol{\theta_6}$	0.2395~ 0.3100	0.4718~ 0.4866	0.0067~ 0.0088	0.0141~ 0.0153	*0.1747~ 0.1910*

4. CONCLUSIONS

An elastic feature-based registration method, along with a tumor mass-effect model, has been presented for the registration of tumor-diseased brains. Moreover, an estimation measure has been proposed for optimization of the corresponding tumor model parameters. After optimization is achieved, the proposed registration method shows reasonably good performance for both the tumor and other brain regions, as validated on simulated and real tumor cases.

5. ACKNOWLEDGEMENTS

This work was supported in part by NIH grant R01 NS042645.

6. REFERENCES

1. A. Mohamed and C. Davatzikos. *Finite Element Modeling of Brain Tumor Mass-Effect from 3D Medical Images*. in MICCAI 2005, Palm Springs, CA.

2. A. Mohamed, *Combining Statistical and Biomechanical Models for Estimation of Anatomical Deformations, Ph.D thesis*, in Computer Science, 2005. Johns Hopkins University: Baltimore.

3. S. Kyriacou, et al., *Nonlinear elastic registration of brain images with tumor pathology using a biomechanical model.* IEEE Trans Medical Imaging, 1999. **18**(7): p. 580-592.

4. B.M. Dawant, S.L. Hartmann, S. Gadamsetty, *Brain Atlas Deformation in the Presence of Large Space-occupying Tumours.* Lect. Notes in Comp. Sci.: MICCAI 1999. **1679**: p. 589-596.

5. M.B. Cuadra, et al., *Atlas-based segmentation of pathological MR brain images using a model of lesion growth.* IEEE Trans Medical Imaging, 2004. **23**(10): p. 1301-1314.

6. O. Clatz, et al., *Realistic Simulation of the 3D Growth of Brain Tumors in MR Images Coupling Diffusion with Mass Effect.* IEEE Trans Medical Imaging, 2005. **24**(10): p. 1334-1346.

7. W.L. Nowinski, D. Belov, *Toward Atlas-Assisted Automatic Interpretation of MRI Morphological Brain Scans in the Presence of Tumor.* Academic Radiology, 2005. **12**(8): p. 1049-1057.

8. D. Shen, C. Davatzikos, *HAMMER: Hierarchical attribute matching mechanism for elastic registration.* IEEE Trans Medical Imaging, 2002. **21**(11): p. 1421-1439.

9. S.M. Smith, *Fast robust automated brain extraction.* Human Brain Mapping, 2002. **17**(3): p. 143-155.

10. D.L. Pham, J.L. Prince, *Adaptive fuzzy segmentation of magnetic resonance images.* IEEE Trans Medical Imaging, 1999. **18**(9): p. 737-752.

11. M. Jenkinson, et al., *Improved optimisation for the robust and accurate linear registration and motion correction of brain images.* NeuroImage, 2002. **17**(2): p. 825-841.

12. Z. Xue, et al. *Statistical Representation and Simulation of High-Dimensional Deformations: Application to Synthesizing Brain Deformations*. in MICCAI. 2005, Palm Springs, California, USA: Springer-Verlag GmbH.